

## Development of a Composite Cu(II)-Selective Potentiometric Sensor Based on a Thiourea Derivative Symmetric Schiff Base

Ozden Yildirim<sup>1</sup>, Fatih Coldur<sup>2\*</sup>, Cihan Topcu<sup>3</sup>, Bulent Caglar<sup>2</sup>

<sup>1</sup>Graduate School of Natural and Applied Sciences, Erzincan Binali Yildirim University, 24100, Erzincan, Turkey.

<sup>2</sup>Department of Chemistry, Faculty of Arts and Sciences, Erzincan Binali Yildirim University, 24100 Erzincan, Turkey.

<sup>3</sup>Department of Biomedical Engineering, Faculty of Engineering, Samsun University, 55420 Ondokuzmayis, Samsun, Turkey.

\*Corresponding author: Fatih Coldur\*, e-mail: [fatihcoldur@hotmail.com](mailto:fatihcoldur@hotmail.com)

Received October 5<sup>th</sup>, 2022; Accepted July 5<sup>th</sup>, 2023.

DOI: <http://dx.doi.org/10.29356/jmcs.v68i2.1884>

**Abstract.** In the present study, initially, a thiourea derivative symmetric Schiff base, (1E,3E)-1,3-bis(5-bromo-2-hydroxybenzylidene)thiourea, was synthesized and characterized by FTIR and SEM-EDX analysis. In addition, an all-solid-state composite Cu(II)-selective potentiometric sensor based on this synthesized compound as an electroactive substance was constructed. Optimization studies indicated that the composition of the optimum sensing composite exhibiting the best potentiometric characteristics was 3.0% Schiff base, 5.0 % multi-walled carbon nanotube (MWCNT), 20.0 % paraffin oil and 72.0% graphite by mass. The proposed sensor displayed a linear response in the concentration range of  $5.0 \times 10^{-6}$ - $1.0 \times 10^{-1}$  M with a slope of 31.1 mV/decade and a detection limit of  $5.0 \times 10^{-7}$  M. The proposed sensor exhibited a fairly selective, stable (potential drift: 1.85 mV/h), and rapid (<10 s) response towards Cu(II) ions. Because of the magnitude of its potential drift, the sensor should be recalibrated along the analysis time at least half an hour apart. The sensor can employed safely in the samples with pHs in the range of 2.0-6.5. The lifetime of the fresh sensor surface was determined as 2 weeks. The most important advantage of the sensor is that the sensing composite surface is renewable (at least 10 times) and thus the sensor can be used many times for a long period of time. The analytical applications of the sensor were executed successfully by using the electrode in the potentiometric titration of Cu(II) ions with EDTA as an indicator electrode, in the direct determination of Cu(II) contents of spiked water samples, and in the determination of (w/w) Cu% content of a Turkish coin.

**Keywords:** Potentiometric sensor; copper(II)-selective electrode; all-solid-state sensor; copper(II) determination; symmetric Schiff base, thiourea derivative.

**Resumen.** En este estudio, inicialmente, se sintetizó una base de Schiff simétrica derivada de la tiourea, (1E,3E)-1,3-bis(5-bromo-2-hidroxibenciliden)tiourea, y se caracterizó mediante análisis FTIR y SEM-EDX. Además, se construyó un sensor potenciométrico selectivo de Cu(II) de estado sólido basado en este compuesto sintetizado como sustancia electroactiva. Los estudios de optimización indicaron que la composición del compuesto sensor óptimo que presentaba las mejores características potenciométricas fue con 3 % de base de Schiff, 5 % de nanotubos de carbono multipared (MWCNT), 20 % de aceite de parafina y 72 % de grafito en masa. El sensor propuesto mostró una respuesta lineal en el rango de concentración de  $5 \times 10^{-6}$  a  $1 \times 10^{-1}$  M con una pendiente de 31 mV/década y un límite de detección de  $5 \times 10^{-7}$  M. El sensor propuesto mostró una respuesta bastante selectiva, estable (deriva de potencial: 1.85 mV/h) y rápida (<10 s) hacia los iones Cu(II). Debido a la magnitud de su deriva de potencial, el sensor debe recalibrarse a lo largo del tiempo de análisis con un intervalo

de al menos media hora. El sensor puede emplearse con seguridad en las muestras con pH en el rango de 2.0 a 6.5. La vida útil de la superficie fresca del sensor se determinó en 2 semanas. La ventaja más importante del sensor es que la superficie del compuesto sensor es renovable (al menos 10 veces) y, por tanto, el sensor puede utilizarse muchas veces durante un largo periodo de tiempo. Las aplicaciones analíticas del sensor se llevaron a cabo con éxito, utilizando el electrodo en la valoración potenciométrica de iones Cu(II) con EDTA como electrodo indicador, en la determinación directa del contenido de Cu(II) de muestras de agua enriquecidas y en la determinación del contenido (p/p) de Cu% de una moneda turca.

**Palabras clave:** Sensor potenciométrico; electrodo selectivo de cobre(II); sensor de estado sólido; determinación de cobre(II); base de Schiff simétrica, derivado de tiourea

---

## Introduction

One of the leading classes of environmental pollutants is heavy metals and they are major pollutants particularly in water pollution. Although several heavy metals at trace levels play essential roles in the survival of organisms, their excessive accumulation in living things has hazardous implications and is one of the primary reasons of the emergence of certain diseases, especially cancer [1].

Due to its high electrical conductivity, chemical stability, plasticity, and capacity to form alloys with numerous metals, copper is used extensively in industrial activities [2]. As a result of these activities, an increasing amount of copper has been discharged into the environment day by day and led to various environmental and health problems. The United States Environmental Protection Agency (EPA) and The World Health Organization (WHO) have set permitted levels for copper in ground water and drinking water at 3 mg/L and 2 mg/L, respectively [3]. The upper tolerable limit for copper in adults is reported as 10 mg per day [4]. High levels of copper exposure might create various health problems such as gastrointestinal distress, anemia, and disruption of liver and renal functions [5]. In particular, the exposure of individuals with Wilson's and Menke's disease to copper is more risky than healthy individuals [6].

Considering the toxic effects of copper, its determination is quite critical. There are a number of analytical techniques that have been reported for the determination of copper ions at very low concentration levels, including ion chromatography [7,8], UV-Vis Spectrophotometry [9,10], flame atomic absorption spectrometry (FAAS) [11,12], graphite-furnace atomic absorption spectrometry (GF AAS) [13], Colorimetry [14-16], fluorescence spectroscopy [17,18], ICP-MS [19], ICP-OES [20], ICP-AES [21], Capillary Electrophoresis-UV [22], titrimetry [23], gravimetry [24], electrogravimetry [25] and electrochemical methods [26-30].

The majority of the above-mentioned techniques take a long time and need the use of environmentally hazardous solvents, complicated pretreatment procedures, special tools, skilled operators, and expensive reagents. Therefore, it is critical to develop a copper detection method that is more efficient, simple, economical, and reliable.

Ion-selective electrodes create an impression as an alternative method to the majority of the aforementioned detection methods for Cu<sup>2+</sup> due to their outstanding features such as high precision and accuracy, broad linear operational range, relatively short analysis time, low limit of detection, adequate selectivity, simple design, cost effectiveness, not to damage the studied samples, mostly no requirement of preprocessing steps, and determinations in colored or turbid solutions [31]. In ionophore-based ISEs, the most critical element controlling the analytical selectivity of the sensor is the chemical substance employed as the ionophore. In the construction of ion-selective electrodes, Schiff bases [32,33], amide derivatives and oxamides [34], crown ethers [35,36], calixarenes [37,38], cryptants [39,40], porphyrins [41,42], metal chelates and ligands [43] are prevalently used as ionophore materials.

Schiff bases, reported first by Hugo Schiff [44], are compounds that bear the imine (-C=N-) functional group. These are condensation products formed by the nucleophilic addition reaction of primary amines with aldehydes and ketones. Schiff bases have been recently used in various fields of application such as corrosion inhibitor [45,46], in the structure of dyestuffs and pigments [47], stabilizers increasing the stability of polymers and light stabilizer in thermoplastic resins [48], ion carriers in polymeric structures [49], in the production of

anticancer, antimicrobial, antifungal and antioxidant substances [50,51], in the developments of fungicide and insecticide in agriculture [52], in the production of cosmetics [53], in perfume [54] and pharmaceutical industry [55].

In recent years, potentiometric sensor technology has made extensive use of all-solid-state composite carbon paste type ion sensors because of their advantages over traditional PVC membrane ion-selective sensors, including the lack of an internal reference solution, robustness and durability, ease of preparation, long life span, renewability, and compatibility with miniaturization. It has also been reported in previous studies that extra improvements in electrochemical performance properties of sensors can be obtained by doping carbon-based nanomaterials (carbon nanotube graphene, etc.) into the sensing carbon paste composite [56,57]. In this study, initially, a novel Schiff base was synthesized and characterized. Later, a composite copper(II)-selective potentiometric sensor based on graphite, carbon nanotubes, paraffin oil, and a currently synthesized symmetric Schiff base as ionophore substance was constructed for the first time for Cu(II) determinations. The potentiometric performance characteristics and analytical applications of the designed sensor were revealed. We believe that the proposed sensor will make a significant contribution to the literature in this area due to its properties as follows: miniaturization, durability, renewability, and performance characteristics comparable to its counterparts.

## Experimental

### Material and reagents

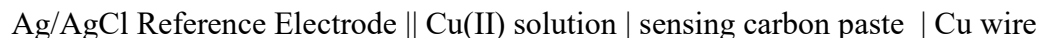
All 5-bromo-salicylaldehyde (5-Br-SA), thiourea (TU), graphite, multi-walled carbon nanotubes (MWCNTs) and paraffin oil were obtained from Sigma-Aldrich (Germany). All the cation solutions used throughout the study were prepared from the nitrate salts of the relevant cations at analytical purity. Deionized water (18.3 MΩ) was used in the preparation of all the solutions.

### Instruments

Potentiometric measurements were performed by a laboratory-made high input impedance computer-controlled potentiometric measurement system. A Gamry (USA) brand saturated Ag/AgCl electrode was used as reference electrode in all potential measurements. All pH measurements were performed with a desktop type Thermo Fisher Scientific (USA) Orion Star A215 pH/Conductivity meter. The FTIR spectra of the samples were attained by a Thermo Nicolet 6700 spectrophotometer in the region of 4000–400  $\text{cm}^{-1}$  using the KBr technique. SEM/EDX data of the samples were obtained from field emission scanning electron microscopy (FE-SEM) (Quanta FEG 450-FEI). ICP-MS analysis were conducted by an Agilent 7700 Series ICP-MS system. The deionized water used along the study was supplied from the Human Corporation Zeener Power II (Korea) water purification system.

### Potentiometric measurements

All potentiometric measurements were recorded at room temperature ( $20 \pm 2$ ) °C. The utilized electrochemical cell assembly for the entire study was as follow:

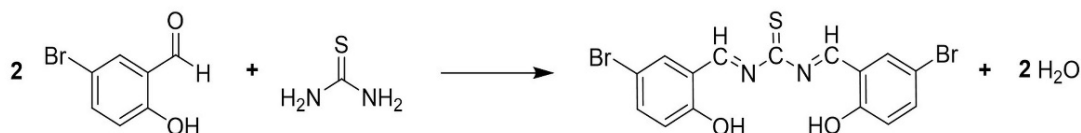


The potentiometric data were collected while the indicator and reference electrodes were immersed in 25 mL of the test solutions, which were stirred at a constant speed. Between measurements, the reference and indicator electrodes were rinsed with deionized water and wiped with soft adsorbent tissue paper.

### Synthesis of (1E,3E)-1,3-bis(5-bromo-2-hydroxybenzylidene)thiourea

The synthesis of thiourea derivative Schiff base (1E,3E)-1,3-bis(5-bromo-2-hydroxybenzylidene)thiourea used as an ionophore in the study was carried out by modifying the synthesis procedure followed by Xinde et al. [58]. For this, 5 mL solutions of thiourea (TU) (0.152 g, 2 mmol) and 5-

bromo-salicylaldehyde (5-Br-SA) (0.804 g, 4 mmol) were combined and mixed at room temperature with the aid of a magnetic stirrer until the final color of the solution turns yellow (72 hours). Later, the pH of the solution was adjusted to 8.0 by incorporating concentrated ammonia solution to the solution. The mixture was stirred again at room temperature for extra 24 hours until a yellow precipitate formed. After removing some of the solvent by distillation, the solution was left to cool. The obtained precipitate was separated by filtration and recrystallized in methanol. The resulting crystals were stored in a desiccator until used. The synthesis reaction of Schiff base is given in Scheme 1.



**Scheme 1.** The synthesis reaction of (1E,3E)-1,3-bis(5-bromo-2-hydroxybenzylidene)thiourea.

### Fabrication of the sensors

The synthesized new Schiff base was used as an electroactive material in the production of all-solid-state composite ion-selective sensors. Potentiometric response of the electrode is created by the complexation reaction between Cu(II) ions and electroactive Schiff base compound present in the sensing composite. Sensing composite component of the sensors were prepared by incorporating graphite, MWCNT, Schiff base and paraffin oil components at different proportions and mixing them well. Then the obtained composites were filled into a teflon tube (inner diameter: 0,4 mm, length: 15 mm) with a conductive wire attached to the other end and pressed. The preparation and general structure of the electrodes are illustrated in Fig. 1. The sensors were conditioned by immersing into  $10^{-2}$  M  $\text{Cu}^{2+}$  solution for 12 hours. The constructed sensors were stored dry under laboratory conditions when not in use. Before starting each measurement process, the sensors were preconditioned in the conditioning solution for at least 1 hour. When the potentiometric behaviour of the sensor was deteriorated, a thin layer of 1mm was removed from the sensor surface with a scalpel and a fresh surface was obtained again. In this way, an electrode surface has the feature of being renewed by cutting 10 times. After the removal of the thin section, the electrode was made ready for measurements by following the same procedures as the newly prepared electrodes. The schematic representation of the potentiometric measurement cell utilized in the current study is as given below:

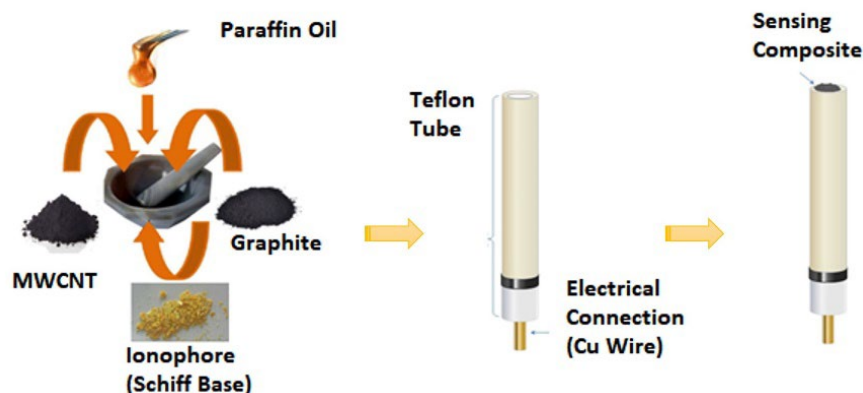
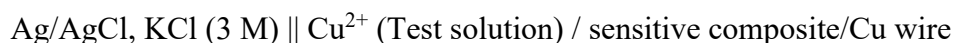


**Fig. 1.** The preparation and general structure of all solid-state composite potentiometric sensors.

## Results and discussion

### Characterizations of synthesized Schiff Base

The FTIR spectra for the starting materials 5-BrSA and TU, as well as the product (1E,3E)-1,3-bis(5-bromo-2-hydroxybenzylidene)thiourea compounds, are demonstrated in Fig. 2.

In the FTIR spectrum of pure 5-BrSA (Fig. 2(a)), O-H stretching at 3230  $\text{cm}^{-1}$ , O-H bending at 1650  $\text{cm}^{-1}$  and C-O stretching bands at 1270  $\text{cm}^{-1}$  are observed. The C-H stretching bands of the aldehyde group on 5-BrSA at 2920, 2877 and 2741  $\text{cm}^{-1}$ ; and the bending band at 1374  $\text{cm}^{-1}$  are observed. The carbonyl (C=O) stretching band of the aldehyde group is quite strong at 1672  $\text{cm}^{-1}$ . In addition, the C-H stretching band at 3045, C=C stretching bands at 1609, 1560 and 1467  $\text{cm}^{-1}$  and out-of-plane bending peaks below 1000  $\text{cm}^{-1}$  which belong to the aromatic ring are observed.

When the FTIR spectrum of pure TU illustrated in Fig. 2(b) is examined, N-H bending band at 1620  $\text{cm}^{-1}$ , N-H stretching bands at 3382, 3276 and 3179  $\text{cm}^{-1}$  belonging to amine group are observed. C-N and C=S stretching vibrations also appear at 1412  $\text{cm}^{-1}$  and 1090  $\text{cm}^{-1}$ , respectively.

When the FTIR spectrum of (1E,3E)-1,3-bis(5-bromo-2-hydroxybenzylidene)thiourea (Fig. 2(c)) which is obtained by the reaction of TU and 5-BrSA at a ratio of 1:2 is examined in detail, the N-H stretching bands at 3382, 3276 and 3179  $\text{cm}^{-1}$ , N-H bending band at 1620  $\text{cm}^{-1}$  originated from TU amine group are disappeared after the synthesis reaction. Similarly, after the reaction, aldehyde C-H stretching bands at 2920, 2877 and 2741  $\text{cm}^{-1}$ , C-H bending band at 1374  $\text{cm}^{-1}$  and strong C=O stretching band at 1672  $\text{cm}^{-1}$  emerged from 5-BrSA are also disappeared. On the other hand, a new C=N stretch band appeared at 1650  $\text{cm}^{-1}$  in the synthesized compound. The appearance of a C=N stretching IR band and disappearances of N-H and C=O stretching IR bands confirm that TU and 5-BrSA combine to form (1E,3E)-1,3-bis(5-bromo-2-hydroxybenzylidene)thiourea Schiff base. Especially, disappearance of N-H stretching vibrations of  $-\text{NH}_2$  groups in TU compound verifies that TU and 5-BrSA are combined in 1:2 stoichiometry (Scheme 1) as an expected chemical structure. In addition to these, the C=C stretch and C-H bending peaks of the aromatic ring in the newly synthesized compound are also observed.

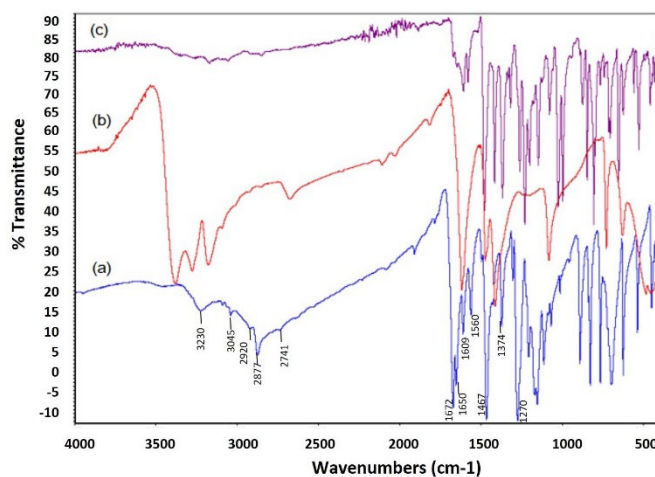
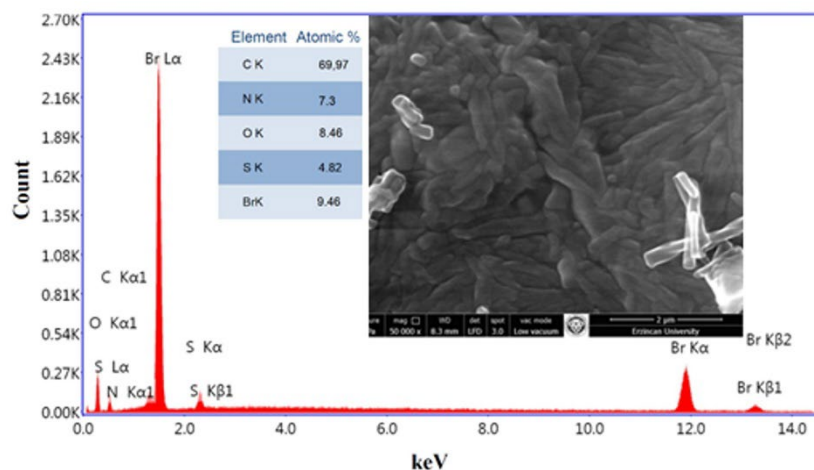


Fig. 2. FTIR spectra of (a) 5-BrSA (b) TU and (c) Schiff base.

SEM-EDX measurements were performed for further characterization of the synthesized compound and the related SEM-EDX data is depicted in Fig. 3.



**Fig. 3.** SEM-EDX analysis of the synthesized Schiff base.

The theoretically calculated atomic percentage values of the C, N, O, S, and Br atoms in the structure of the compound are 68.18, 9.09, 9.09, 4.55, and 9.09, respectively. The values obtained by EDX measurements for the interested elements are 69.97, 7.3, 8.46, 4.82, and 9.46, respectively. According to EDX analyses, the atomic percentage values of N, O, and Br atoms are nearly two times greater than that of the S atom. Additionally, the atomic percentage value of the C atom is approximately 15 times greater than that of the S atom. These results endorse that the compound obtained in the synthesis reaction has the expected chemical structure.

### Optimization of the sensor composition

In potentiometric ion selective sensors, it is familiar that the structural composition of the sensing unit tremendously influences the performance properties of the sensor. For this reason, composition of the composite sensing unit displaying the best performance properties was scrutinized by studying the different incorporation ratios of the components. The studied electrode compositions and a summary of some certain potentiometric performance characteristics belonging to them were provided in Table 1 and Table 2, respectively.

Initially, the influence of the paraffin oil ratio in the composite membrane structure on the potentiometric performance properties of the sensor was investigated. For this purpose, the sensors containing a fixed ionophore content of (w/w) 5.0 % were prepared using graphite and varying amounts of paraffin oil (Composition 1-4). The data in Table 2 indicate that the best potentiometric performance characteristics are obtained when (w/w) 20.0 % of paraffin oil is used in the composite structure (Composition 3). In addition, the effect of MWCNT ratio used in the membrane structure on the potentiometric behaviour of the sensor was investigated. Inevitably, the electrodes were produced by using the compositions containing graphite and MWCNT in various ratios by keeping the paraffin oil ratio constant at (w/w) 20.0% (Composition 1-4). The potentiometric performance characteristics of the sensors given in Table 2 show that the membrane with the best performance in terms of MWCNT ratio is the one containing (w/w) 5.0 % of MWCNT (Composition 7). In the following section of the optimization study, the influence of the ionophore percent by mass on the final performance properties of the sensor was investigated. To this end, a series of composites were prepared by using ionophore material at varying mass percentages by keeping the paraffin oil and the MWCNT ratio constant at (w/w) 20.0 % and (w/w) 5.0, respectively (Composition 7, 10-12). The calculated performance characteristics indicate that the composition containing (w/w) 3.0 % ionophore (Composition 10) exhibits the best potentiometric performance properties in terms of ionophore ratio. In the last part of the optimization studies, the influence of the ionic additive percentage on the sensor performance was examined. Therefore, a series of all-solid-state composite electrodes were

produced by adding ionic additives in the ratios varying between (w/w) 0.5-2.5 % to the composition of (w/w) 20.0 % paraffin oil, (w/w) 5.0 % MWCNT, and (w/w) 3.0 % ionophore (NaTPB) (Composition 13-17) and their performance characteristics were compared. The data given in Table 2 indicate that none of the studied compositions including ionic additive had any preemptory effect on the electrode performances. All these membrane optimization studies indicate that the sensor composition exhibiting the best potentiometric performance properties among the studied membranes consists of (w/w) 3.0 % ionophore, (w/w) 5.0 % MWCNT, (w/w) 20.0 % paraffin oil and (w/w) 72.0 % graphite. The following section takes a closer look at the potentiometric performance characteristics of the sensor prepared on the bases of the optimum composition.

**Table 1.** The examined sensor compositions in the optimization study.

Compositions	(w/w) %				
	Ionophore	Graphite	MWCNT	Paraffin Oil	Ionic Additive (NaTPB)
1	5.0	65.0	-	30.0	-
2	5.0	70.0	-	25.0	-
3	5.0	75.0	-	20.0	-
4	5.0	80.0	-	15.0	-
5	5.0	74.0	1.0	20.0	-
6	5.0	72.0	3.0	20.0	-
7	5.0	70.0	5.0	20.0	-
8	5.0	65.0	10.0	20.0	--
9	10.0	65.0	5.0	20.0	-
10	3.0	72.0	5.0	20.0	
11	2.0	73.0	5.0	20.0	-
12	1.0	74.0	5.0	20.0	-
13	3.0	71.5	5.0	20.0	0.5
14	3.0	71.0	5.0	20.0	1.0
15	3.0	70.5	5.0	20.0	1.5
16	3.0	70.0	5.0	20.0	2.0
17	3.0	69.5	5.0	20.0	2.5

**Table 2.** Some of the performance characteristics of the sensors prepared in the investigated membrane compositions.

Compositions	Slope, mV/decade	Detection Limit, M	Linear Range, M	R <sup>2</sup>
1	20.3	1.0×10 <sup>-4</sup>	1.0×10 <sup>-3</sup> -1.0×10 <sup>-1</sup>	0.9981
2	21.8	1.0×10 <sup>-4</sup>	5.0×10 <sup>-4</sup> -1.0×10 <sup>-1</sup>	0.9943
3	24.4	5.0×10 <sup>-5</sup>	1.0×10 <sup>-4</sup> -1.0×10 <sup>-1</sup>	0.9987
4	21.2	1.0×10 <sup>-4</sup>	5.0×10 <sup>-4</sup> -5.0×10 <sup>-2</sup>	0.9921
5	25.0	1.0×10 <sup>-5</sup>	3.0×10 <sup>-5</sup> -1.0×10 <sup>-1</sup>	0.9966
6	28.3	8.0×10 <sup>-6</sup>	1.0×10 <sup>-5</sup> -1.0×10 <sup>-1</sup>	0.9972
7	28.5	2.0×10 <sup>-6</sup>	1.0×10 <sup>-5</sup> -1.0×10 <sup>-1</sup>	0.9973
8	27.1	5.0×10 <sup>-6</sup>	1.0×10 <sup>-5</sup> -1.0×10 <sup>-2</sup>	0.9949
9	23.5	5.0×10 <sup>-5</sup>	1.0×10 <sup>-4</sup> -1.0×10 <sup>-2</sup>	0.9968
10	31.1	5.0×10 <sup>-7</sup>	5.0×10 <sup>-6</sup> -1.0×10 <sup>-1</sup>	0.9959
11	29.7	9.0×10 <sup>-7</sup>	7.0×10 <sup>-6</sup> -1.0×10 <sup>-1</sup>	0.9924
12	28.9	1.0×10 <sup>-6</sup>	8.0×10 <sup>-6</sup> -1.0×10 <sup>-2</sup>	0.9924
13	26.2	8.0×10 <sup>-6</sup>	1.0×10 <sup>-5</sup> -1.0×10 <sup>-2</sup>	0.9986
14	27.8	8.0×10 <sup>-6</sup>	2.0×10 <sup>-5</sup> -1.0×10 <sup>-2</sup>	0.9962
15	27.4	7.0×10 <sup>-6</sup>	2.0×10 <sup>-5</sup> -1.0×10 <sup>-2</sup>	0.9977
16	29.0	8.0×10 <sup>-6</sup>	1.0×10 <sup>-5</sup> -5.0×10 <sup>-3</sup>	0.9938
17	28.9	6.0×10 <sup>-6</sup>	1.0×10 <sup>-5</sup> -5.0×10 <sup>-3</sup>	0.9943

### Potentiometric performance characteristics of the optimum sensor composition

In order to reveal the potentiometric performance characteristics of the developed Cu<sup>2+</sup>-selective electrode in detail, a series of potentiometric measurements were taken in standard Cu<sup>2+</sup> solutions in the concentration range of 1.0×10<sup>-1</sup>–1.0×10<sup>-8</sup> M. The obtained potentiometric response curve, calibration curve and linear calibration plot were created and depicted in Fig. 4. The potentiometric response of the electrode fits the mathematical equation of  $E=31,136.\log[\text{Cu}^{2+}]+2769,2$ . The electrode exhibits a linear response to Cu<sup>2+</sup> ions in the concentration range of 5.0×10<sup>-6</sup>-1.0×10<sup>-1</sup> M with a slope of 31.1 mV/decade and a detection limit of 5.0×10<sup>-7</sup> M calculated according to the IUPAC recommendations [59]. As could be seen, the suggested electrode exhibits a near-Nernstian response to Cu<sup>2+</sup> ions.

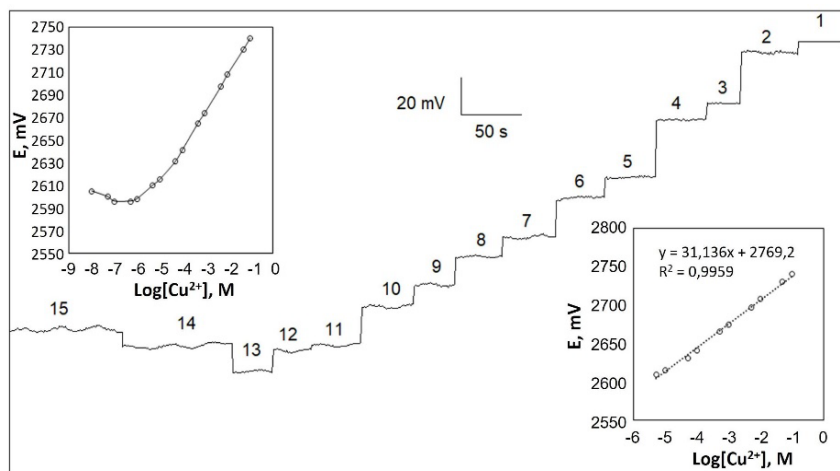


**Fig. 4.** The potentiometric responses of the sensor in  $\text{Cu}^{2+}$  solutions at different concentrations, the corresponding response curve (upper left inset), and the calibration graph (bottom right inset) in the linear operating range. (1:  $1,0 \times 10^{-1}$  M, 2:  $5,0 \times 10^{-2}$  M, 3:  $1,0 \times 10^{-2}$  M, 4:  $5,0 \times 10^{-3}$  M, 5:  $1,0 \times 10^{-3}$  M, 6:  $5,0 \times 10^{-4}$  M, 7:  $1,0 \times 10^{-4}$  M, 8:  $5,0 \times 10^{-5}$  M, 9:  $1,0 \times 10^{-5}$  M, 10:  $5,0 \times 10^{-6}$  M, 11:  $1,0 \times 10^{-6}$  M, 12:  $5,0 \times 10^{-7}$  M, 13:  $1,0 \times 10^{-7}$  M, 14:  $5,0 \times 10^{-8}$  M, 15:  $1,0 \times 10^{-8}$  M).

Real-time measurements were taken from low concentration to high concentration and vice versa in standard  $\text{Cu}^{2+}$  solutions while the potentiometric system was continuously collecting data to determine the response time of the sensor. Fig. 5 depicts the time required for the sensor response to reach equilibrium during transitions between solutions at varying concentrations. The response time of the sensor was calculated as  $t_{95}$  for each concentration change, as recommended by IUPAC [59]. Taking the average of these calculated  $t_{95}$  values yielded the sensor's average response time. It is seen that the sensor responds quickly enough to the concentration changes of  $\text{Cu}^{2+}$  ions and reaches equilibrium in a short time. It was determined that the average response time of the sensor calculated at the studied concentrations was  $<10$  s.

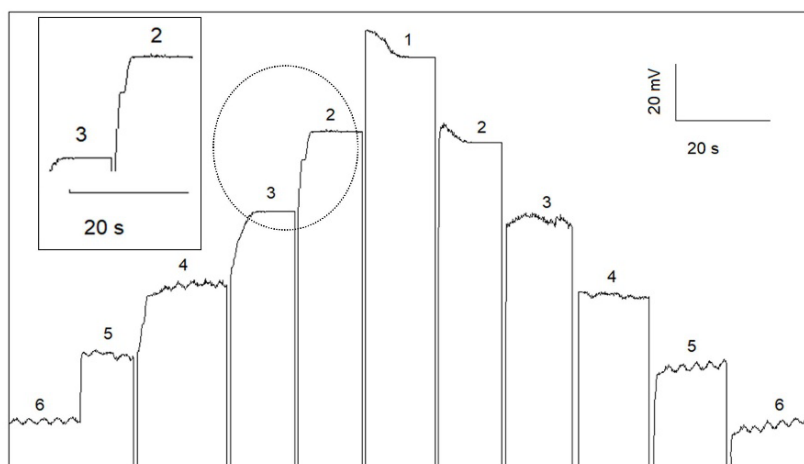


**Fig. 5.** Response time of the suggested  $\text{Cu}^{2+}$ -selective sensor. (1:  $1,0 \times 10^{-1}$  M 2:  $1,0 \times 10^{-2}$  M 3:  $1,0 \times 10^{-3}$  M 4:  $1,0 \times 10^{-4}$  M, 5:  $1,0 \times 10^{-5}$  M, 6:  $1,0 \times 10^{-6}$  M).

To have an idea about the repeatability of the sensor response, repeated measurements were taken in  $1.0 \times 10^{-5}$ ,  $1.0 \times 10^{-4}$  and  $1.0 \times 10^{-3}$  M  $\text{Cu}^{2+}$  solutions (Fig. 6). The mean and standard deviations of the potential values obtained from the repeated measurements carried out in  $1.0 \times 10^{-5}$ ,  $1.0 \times 10^{-4}$  and  $1.0 \times 10^{-3}$  M  $\text{Cu}^{2+}$  solutions were figured out as  $2613.6 \pm 2.5$ ,  $2641.3 \pm 0.6$  and  $2670.6 \pm 0.3$  respectively. In addition to repeatability studies of the proposed electrode, the reproducibility of the electrode behavior depending on the surface regeneration was also investigated. Three fresh surfaces were created on the same electrode by removing 1 mm sections from its surface each time. After each new surface was obtained, the surfaces were conditioned by following the conditioning process of a new electrode and related calibration lines were created in standard copper(II) solutions (in the range of  $5.0 \times 10^{-6}$ - $1.0 \times 10^{-1}$  M). The calibration lines obtained for each fresh surface are illustrated in Fig. 7. As can be seen the slope values belonging to each fresh surface changed between 30.95 and 31.92 mV/decade which indicates that the potentiometric behaviour of the electrode remains nearly unchanged. However, it should be noted that although there is not much change in the slope of the electrode depending on surface renewal, there is a shift in the initial potentials of the calibration lines. Therefore, it seems imperative to recalibrate the electrode after each surface renewal.

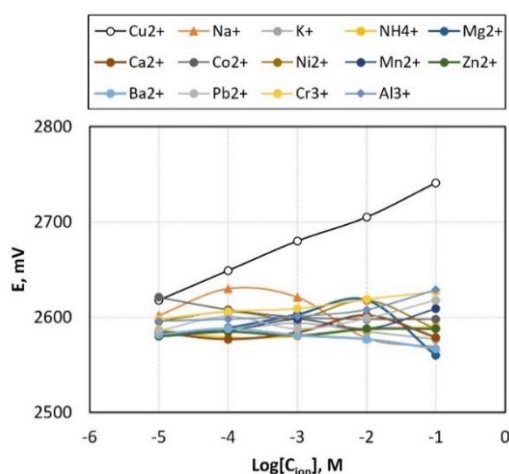


Fig. 6. Repeatability of the sensor in  $\text{Cu}^{2+}$  solutions at different concentrations.

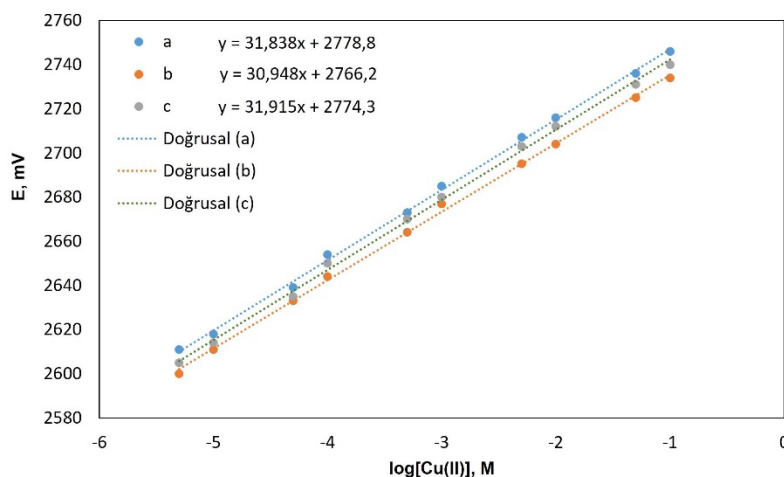
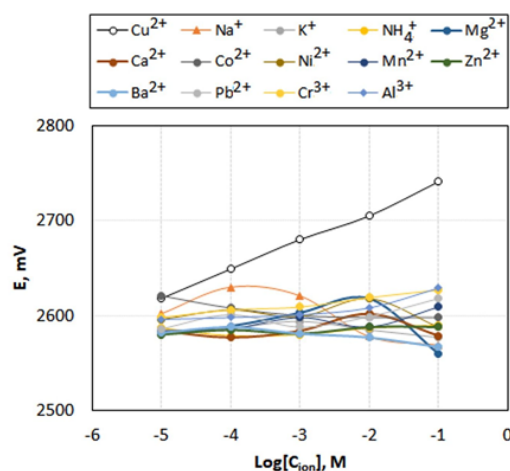


Fig. 7. Potentiometric response plots of the  $\text{Cu}^{2+}$ -selective electrode depending on surface renewal.

To expose the selective behaviour of the sensor toward  $\text{Cu}^{2+}$  in comparison to other ionic species, potentiometric signals in  $\text{Cu}^{2+}$  and other ionic species solutions at various concentrations were recorded. The potentiometric response curves attained against the concentrations of the solutions are shown in Fig. 8. When Fig. 8 is examined, it is noteworthy that the response of the sensor to  $\text{Cu}^{2+}$  distinguishes significantly from the response of the other studied ionic species. The selectivity coefficients for each examined ionic species were computed using the Separate Solution Method [60] and reported in Table 3 in order to quantitatively express the selectivity of the sensor.



**Fig. 8.** The potentiometric response of the  $\text{Cu}^{2+}$ -selective sensor in solutions of different ions at different concentrations.

**Table 3.** Selectivity coefficients were calculated according to the Separate Solution Method (SSM) for some studied species.

Ion (X)	$\log K_{\text{Cu(II),X}}$	Ion (X)	$\log K_{\text{Cu(II),X}}$
$\text{Cu}^{2+}$	0.00	$\text{Ni}^{2+}$	-3.01
$\text{Na}^+$	-2.33	$\text{Mn}^{2+}$	-4.30
$\text{K}^+$	-2.10	$\text{Zn}^{2+}$	-4.00
$\text{NH}_4^+$	-3.93	$\text{Ba}^{2+}$	-4.36
$\text{Mg}^{2+}$	-3.01	$\text{Pb}^{2+}$	-4.01
$\text{Ca}^{2+}$	-3.54	$\text{Cr}^{3+}$	-4.04
$\text{Co}^{2+}$	-3.67	$\text{Al}^{3+}$	-3.98

Table 3 shows that  $\text{K}^+$ ,  $\text{Na}^+$ , and  $\text{Ni}^{2+}$ , in that order, are the most significant ions that interfere with  $\text{Cu}^{2+}$  ions. Even when compared to the most interfering  $\text{K}^+$  ion, the electrode is more selective to  $\text{Cu}^{2+}$  ions more than 100 times.

In order to determine the useful pH operating range of the electrode, potential measurements were recorded in the standard solutions containing  $1.0 \times 10^{-3}$  and  $1.0 \times 10^{-4}$  M fixed  $\text{Cu}^{2+}$  and different  $\text{H}_3\text{O}^+$  ion

concentrations (pH=0.5-11.6). The pH of the solutions was adjusted by adding a few drops of concentrated HCl and NaOH solutions. The pH profile of the electrode was obtained by plotting the relevant potential values against the solution pHs (Fig. 9). The potential values of the sensor against  $\text{Cu}^{2+}$  ions in the pH range of 2.0-6.5 are strikingly unaffected by pH changes when the graph in Fig. 9 is inspected. It is observed that as the pH levels of the solutions go below 2.0, the electrode potential begins to rise dramatically. This can be explained by the fact that the selective composite begins to respond to increasing hydronium ions along with the copper ions. When the pH of the solution exceeds 6.5, the electrode potential begins rapidly decrease, as expected. We believe that this situation is related to the decrease in Cu(II) concentration through complex formation with  $\text{OH}^-$  ions of  $\text{Cu}^{2+}$  ions in the environment as the  $\text{OH}^-$  concentration increases.

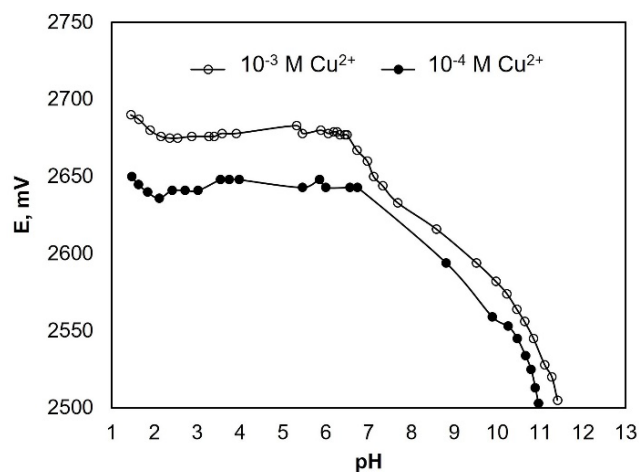


**Fig. 9.** Variation of the potentiometric response of the  $\text{Cu}^{2+}$ -selective electrode depending on the pH of the measurement medium.

It is preferable for any sensor's response to remain stable and constant as long as the conditions do not change. Based on this situation, we investigated the signal stability of the currently proposed sensor. The electrode and the reference electrode were immersed into  $1.0 \times 10^{-3}$  M  $\text{Cu}^{2+}$  solution and the potential of the electrochemical cell was recorded over time for 11 hours. The recorded potentials over time is demonstrated in Fig. 10. As can be seen, a total of 20.6 mV shift is observed in the potential of the electrode in  $1.0 \times 10^{-3}$  M  $\text{Cu}^{2+}$  solution at the end of the 11 hours period (1.85 mV/h). This magnitude of potential shift indicates that the sensor response is sufficiently stable. At this point, it should be emphasized that a potential shift of 1.85 mV per hour can lead to a significant error (approximately 3.0 % at logarithmic scale) in the determinations when the same calibration curve is used after one hour. This is valid when the electrode is constantly in contact with the solution for 1 hour. As a result, calibrating the electrode before each determination process will lead to more accurate and reliable analysis results.

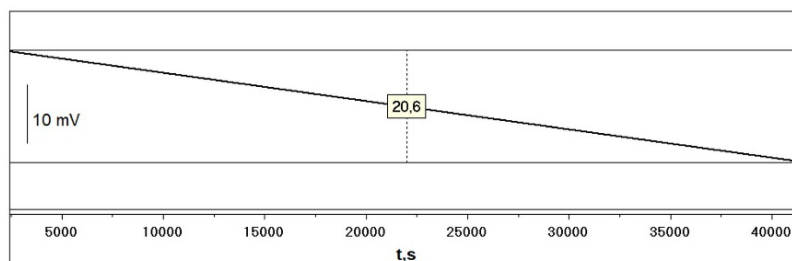


**Fig. 10.** The observed potential shift in the response of the  $\text{Cu}^{2+}$ -selective sensor over 11 hours in  $1.0 \times 10^{-3}$  M  $\text{Cu}^{2+}$  solution.

The slope of the potentiometric response in the concentration range of  $5.0 \times 10^{-6}$ – $1.0 \times 10^{-1}$  M was monitored daily to determine the useful life-time of the proposed sensor. Fig. 11 depicts the changes in the calculated slope values depending on time. The slope value of the sensor (19.0 mV/ten-fold concentration change) fell below 70 % of the initial slope value (31.1 mV/ten-fold concentration change) after the 14th day, as seen in the graph. Thereof, the life-time of a new surface on the composite sensor is about 2 weeks. This value is approximate and may vary depending on frequency of use. The lifetime of the sensor may seem very short, but the fact that the surface of the composite sensor prepared in this study is constantly renewed by removing a thin section from the surface. This way of use can provide a much longer operational life-time for an existing sensor. This is one of the most significant benefits of the proposed composite membrane sensor.

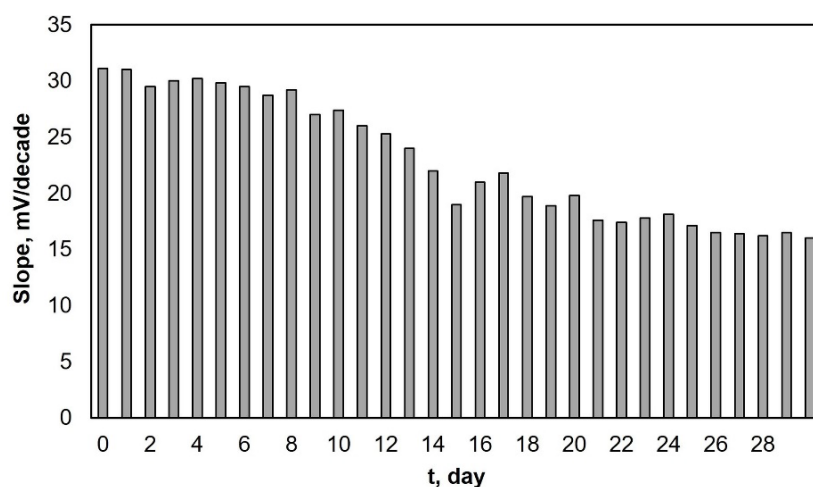


**Fig. 11.** Time-dependent change in the slope of the  $\text{Cu}^{2+}$ -selective sensor in the linear working range.

### Analytical applications

Several analytical applications of the recommended sensor were performed to demonstrate its analytical usefulness. The sensor was initially used as an indicator electrode for the titration of  $\text{Cu}^{2+}$  ions with EDTA. Throughout the titration process, the measured potential values of the solution were recorded by the potentiometric system while slowly adding  $1.0 \times 10^{-2}$  M EDTA solution in small volumes to continuously stirred  $1.0 \times 10^{-3}$  M 25 mL  $\text{Cu}^{2+}$  solution. The obtained titration curve was illustrated in Fig. 12. Because the  $\text{Cu}^{2+}$  ion concentration decreased in the medium with each addition of EDTA to the solution, as a consequence of the complexation reaction, the potential values gradually decreased in the later stages of titration process. Using the portion of the titration curve where the sudden drop in potential occurred, the potentiometric end-point of the titration was calculated as 2.6 mL. ( $V_{\text{theoretical}}=2.5$  mL).

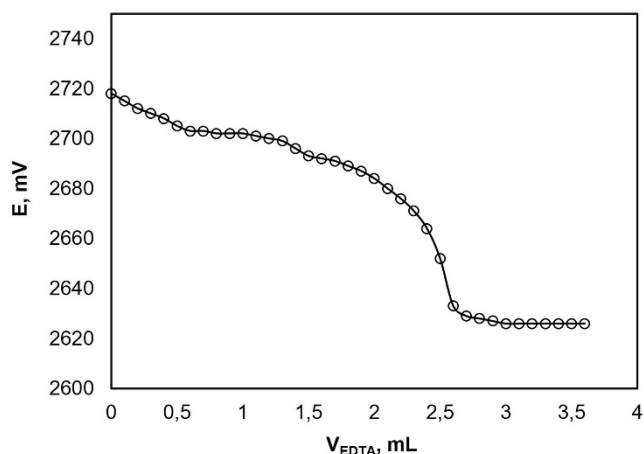


**Fig. 12.** Titration curve obtained from potentiometric titration of 25 mL  $1.0 \times 10^{-3}$  M  $\text{Cu}^{2+}$  solution with  $1.0 \times 10^{-2}$  M EDTA solution.

In another analytical application of the present sensor, Cu(II) determinations were carried out directly in tap water samples into which Cu(II) ions were spiked at concentrations ranging between  $1.0 \times 10^{-1}$ - $1.0 \times 10^{-4}$  M. The actual  $\text{Cu}^{2+}$  concentrations in the solutions, the estimated  $\text{Cu}^{2+}$  concentrations by the potentiometric method and regarding recovery values were given in Table 4. As can be seen, fairly good recovery values ranging from 98-111 % were obtained.

**Table 4.** Direct potentiometric determinations of  $\text{Cu}^{2+}$  ions in spiked tap water samples by the proposed electrode.

Water samples	Actual $[\text{Cu}^{2+}]$ , M	Estimated $[\text{Cu}^{2+}]$ , M (N=3)	% RSD	Recovery
1	$4.0 \times 10^{-4}$	$4.5 \pm 0.3 \times 10^{-4}$	7.8	111
2	$2.0 \times 10^{-3}$	$2.1 \pm 0.1 \times 10^{-3}$	4.4	103
3	$3.0 \times 10^{-3}$	$3.1 \pm 0.1 \times 10^{-3}$	3.9	104
4	$4.0 \times 10^{-2}$	$3.9 \pm 0.2 \times 10^{-2}$	4.6	98
5	$6.0 \times 10^{-2}$	$6.2 \pm 0.1 \times 10^{-2}$	2.3	102

With regard to the final analytical use of the sensor, the copper percentage of a Turkish coin (25 kuruş, year: 2009) was determined by using the proposed sensor. For this purpose, initially, about 0.4 g of coin was completely dissolved in 10 mL of concentrated nitric acid, the resulting mixture was heated to dryness and then diluted to a final volume of 1000 mL with de-ionized water. Sample solution prepared by diluting the main sample solution in appropriate proportion was implemented for the determinations carried out by potentiometry and ICP-MS. Before the potentiometric determination, pH of the analysed solution was adjusted to 5.0 with the addition of small amount of NaOH solution. Standard addition method was used in the potentiometric determination to eliminate errors brought on by the matrix. While the reported theoretical Cu percent by weight is 60.0, the determined Cu percent for potentiometry and ICP-MS are  $61.3 \pm 0.3$  and  $59.7 \pm 0.2$ , respectively for 5 replications. In this case, the calculated recovery % value for potentiometric determination with respect to

ICP-MS determination is 102.7. The most striking and impressive aspect of these results is that the standard deviation values of the ICP-MS results and the potentiometric results are almost the same. This shows that the repeatability of potentiometric measurements in this application is almost at the same level as that of ICP-MS measurements. These results verify that the recently recommended all-solid-state composite Cu<sup>2+</sup>-selective sensor can be successfully and practically used for Cu<sup>2+</sup> determination in this sort of real samples as an alternative to more sophisticated systems.

## Conclusions

To some up, a novel potentiometric all-solid-state composite Cu<sup>2+</sup>-selective sensor based on a thiourea derivative symmetric Schiff base, (1E,3E)-1,3-bis(5-bromo-2-hydroxybenzylidene)thiourea, was favourably developed and employed for Cu<sup>2+</sup> determinations. Along the study, it was shown that the sensor had a high affinity to Cu<sup>2+</sup> ions in a wide linear range with a well-nigh Nernstian behaviour. In terms of stability, response time, life-time, pH range and selectivity, very satisfactory potentiometric performance characteristics were obtained. The proposed sensor was successfully applied as the indicator electrode for the determination of Cu<sup>2+</sup> ions by the titration of EDTA. It was also satisfactorily used for the determination of Cu<sup>2+</sup> contents of some spiked tap water samples and (w/w) Cu% content of Turkish coins. One of the most striking advantages of the sensor is that the regeneration of the sensor surface can be achieved by the removal of a thin section from the sensing surface and can be used time and again, due to its structural nature. The sensor is sufficiently robust and particularly ideal for miniaturization purposes. The proposed sensor can be preferred for rapid, accurate, practical and cheap determinations of Cu<sup>2+</sup> levels at various sample types in the future.

## Acknowledgements

The authors express their deep gratitude to the Management of Faculty of Arts and Sciences (Erzincan Binali Yildirim University) because of the provided facilities and opportunities to achieve the study.

## References

1. Jaishankar, M.; Tseten, T.; Anbalagan, N.; Mathew, B.B.; Beeregowda, K.N. *Interdiscip. Toxicol.* **2014**, 7, 60–72. DOI: <https://doi.org/10.2478/intox-2014-0009>.
2. Richardson, H.W., in: *Handbook of Copper Compounds and Applications*. Marcel Dekker, New York, **1997**.
3. Institute of Medicine (US) Panel on Micronutrients. Dietary Reference Intakes for Vitamin A, Vitamin K, Arsenic, Boron, Chromium, Copper, Iodine, Iron, Manganese, Molybdenum, Nickel, Silicon, Vanadium, and Zinc. Washington (DC): National Academies Press (US); 2001. 7, Copper. Available from: <https://www.ncbi.nlm.nih.gov/books/NBK222312/>
4. Hordyjewska, A.; Popiolek, L.; Kocot, J. *Biomaterials*. **2014**, 27, 611–621. DOI: <https://doi.org/10.1007/s10534-014-9736-5>.
5. Schaefer, M.; Gitlin, G. D. *Am. J. Physiol. Gastrointest. Liver Physiol.* **1999**, 276, G311–G314. DOI: <https://doi.org/10.1152/ajpgi.1999.276.2.G311>.
6. Ali, A.; Shen, H.; Yin, X. *Anal. Chim. Acta.* **1998**, 369, 215–223. DOI: [https://doi.org/10.1016/S0003-2670\(98\)00252-9](https://doi.org/10.1016/S0003-2670(98)00252-9).
7. Bruno, P.; Caselli, M.; Daresta, B. E.; de Gennaro G.; de Pinto, V.; Ielpo, P.; Placentino C. M. *J. Liq. Chromatogr. Relat. Technol.* **2007**, 30, 477–487. DOI: <https://doi.org/10.1080/10826070601093762>.
8. Yaseen, S.; Qasim, B.; Al-lame, N. *Egypt. J. Chem.* **2021**, 64, 673–691. DOI: <https://doi.org/10.21608/ejchem.2019.13907.1861>.

9. Babayeva, K.; Demir, S.; Andac, M. *J. Taibah Univ. Sci.*, **2017**, *11*, 808–814. DOI: <https://doi.org/10.1016/j.jtusci.2017.02.001>.
10. Arpa Şahin, Ç.; Tokgöz, İ. *Anal. Chim. Acta* **2010**, *667*, 83–87. DOI: <https://doi.org/10.1016/j.aca.2010.04.012>.
11. Bagherian, G.; Arab Chamjangali, M.; Shariati Evvari, H.; Ashrafi, M. *J. Anal. Sci. Technol.* **2019**, *10*, 3. DOI: <https://doi.org/10.1186/s40543-019-0164-6>.
12. Neri, T. S.; Rocha, D. P.; Muñoz, R. A. A.; Coelho, N. M. M.; Batista, A. D. *Microchem. J.*, **2019**, *147*, 894–898. DOI: <https://doi.org/10.1016/j.microc.2019.04.014>.
13. Erdoğan, H. *Düzce Üniversitesi Bilim ve Teknoloji Dergisi.* **2021**, *9*, 1469–1482. DOI: <https://doi.org/10.29130/dubited.884511>.
14. Poosinuntakul, N.; Parnklang, T.; Sitiwed, T.; Chaiyo, S.; Kladsomboon, S.; Chailapakul, O.; Apilux, *Microchem. J.*, **2020**, *158*, 105101. DOI: <https://doi.org/10.1016/j.microc.2020.105101>.
15. Clark, A. C.; Zhang, X.; Kontoudakis, N. *Aust. J. Grape Wine Res.* **2020**, *26*, 399–409. <https://doi.org/10.1111/ajgw.12450>.
16. Vasimalai, N.; Prabhakarn, A.; Abraham John, S. *Nanotechnology.* **2013**, *24*, 505503. DOI: <https://doi.org/10.1088/0957-4484/24/50/505503>.
17. He, L.; Bao, Z.; Zhang, K.; Yang, D.; Sheng, B.; Huang, R.; Zhao, T.; Liang, X.; Yang, X.; Yang, A.; Zhang, C.; Cui, P.; Zapfen, J. A.; Zhou, H. *Microchim. Acta.* **2018**, *185*, 511. DOI: <https://doi.org/10.1007/s00604-018-3043-8>.
18. Chrastný, V.; Komárek, M. *Chem. Pap.* **2009**, *63*, 512–519. DOI: <https://doi.org/10.2478/s11696-009-0057-z>.
19. Yilmaz, V.; Arslan, Z.; Hazer, O.; Yilmaz, H. *Microchem. J.* **2014**, *114*, 66–72. DOI: <https://doi.org/10.1016/j.microc.2013.12.002>.
20. Ferreira, S. L.; Santos, H. C.; Ferreira, J. R.; Araujo, N. M.; Costa, A. C.; Jesus, D. S. *J. Braz. Chem. Soc.* **1998**, *9*, 525–530. DOI: <https://doi.org/10.1590/S0103-50531998000600004>.
21. Basheer, C.; Lee, H. K.; *Electrophoresis.* **2007**, *28*, 3520–3525. DOI: <https://doi.org/10.1002/elps.200700248>.
22. Ergün, E. G. C.; Kenar, A. *Turk. J. Chem.* **2018**, *42*, 257–263. DOI: <https://doi.org/10.3906/kim-1703-83>.
23. Uesugi, K.; Kumagai, T.; Wada, S. *Microchem. J.* **1986**, *33*, 204–208. DOI: [https://doi.org/10.1016/0026-265X\(86\)90056-1](https://doi.org/10.1016/0026-265X(86)90056-1).
24. Musa, D.; Sha’Ato, R.; Eneji, I.; Itodo, A. *Open Access Library Journal.* **2018**, *5*, 1–14. DOI: <https://doi.org/10.4236/oalib.1104446>.
25. Topcu, C.; Lacin, G.; Yilmaz, V.; Coldur, F.; Caglar, B.; Cubuk, O.; Isildak, I. *Anal. Lett.* **2018**, *51*, 1890–1910. DOI: [10.1080/00032719.2017.1395035](https://doi.org/10.1080/00032719.2017.1395035).
26. Mohammadi, S.; Taher, M. A.; Beitollahi, H. *Russ. J. Electrochem.* **2021**, *57*, 1175–1185. DOI: <https://doi.org/10.1134/S1023193521100098>.
27. Cui, Y.; Yang, C., in: *3rd International Conference on Bioinformatics and Biomedical Engineering*, **2009**, 1–4. DOI: <https://doi.org/10.1109/ICBBE.2009.5162761>.
28. Romero-Cano, L. A.; Zárate-Guzmán, A. I.; Carrasco-Marín, F.; González-Gutiérrez, L. V. *J. Electroanal. Chem.* **2019**, *837*, 22–29. DOI: <https://doi.org/10.1016/j.jelechem.2019.02.005>.
29. Chong, J. M.; Nor, A. Y.; Shahrul Ainliah, A. A. *Chemosensors.* **2021**, *9*, 157. DOI: <https://doi.org/10.3390/chemosensors9070157>.
30. Khalil, S.; El-Sharnouby, M. *Chemosensors.* **2021**, *9*, 86. DOI: <https://doi.org/10.3390/chemosensors9050086>.
31. Mashhadizadeh, M. H.; Sheikhshoae, I. *Talanta.* **2003**, *60*, 73–80. DOI: [https://doi.org/10.1016/S0039-9140\(03\)00036-5](https://doi.org/10.1016/S0039-9140(03)00036-5).
32. Ganjali, M. R.; Emami, M.; Rezapour, M.; Shamsipur, M.; Maddah, M.; Salavat-Niasari, M.; Hosseini, M.; Talebpour, Z. *Anal. Chim. Acta.* **2003**, *495*, 51–59. DOI: [https://doi.org/10.1016/S0003-2670\(03\)00921-8](https://doi.org/10.1016/S0003-2670(03)00921-8).
33. Malinowska, E. *Analyst.* **1990**, *115*, 1085–1087. DOI: <https://doi.org/10.1039/AN9901501085>.
34. Ganjali, M. R.; Roubollahi, A.; Mardan, A. R.; Hamzeloo, M.; Mogimi, A.; Shamsipur, M. *Microchem. J.* **1998**, *60*, 122–133. DOI: <https://doi.org/10.1006/mchj.1998.1642>.
35. Su, C. C.; Chang, M. C.; Liu, L. K. *Anal. Chim. Acta.* **2001**, *423*, 261–267. DOI: [https://doi.org/10.1016/S0003-2670\(00\)01375-1](https://doi.org/10.1016/S0003-2670(00)01375-1).

36. Gupta, V. K.; Mangla, R.; Aggarwal, S. *Electroanalysis*. **2002**, *14*, 1127. DOI: [https://doi.org/10.1002/1521-4109\(200208\)14:15/16<1127::AID-ELAN1127>3.0.CO;2-7](https://doi.org/10.1002/1521-4109(200208)14:15/16<1127::AID-ELAN1127>3.0.CO;2-7)
37. Bhat, V. S.; Ijeri, V. S.; Srivastava, A. K. *Sens. Actuat.* **2004**, *99*, 98–105. DOI: <https://doi.org/10.1016/j.snb.2003.11.001>.
38. Amini, M. K.; Mazloum, M.; Ensafi, A. A. *Fresenius J. Anal. Chem.* **1999**, *364*, 690–693. DOI: <https://doi.org/10.1007/s002160051415>.
39. Srivastava, S. K.; Gupta, V. K.; Jain, S. *Anal. Chem.* **1996**, *68*, 1272–1275. DOI: <https://doi.org/10.1021/ac9507000>.
40. Ardakani, M. M.; Dehghani, H.; Jalayer, M. S.; Zare, H. R. *Anal. Sci.* **2004**, *20*, 1667–1672. DOI: <https://doi.org/10.2116/analsci.20.1667>.
41. Yagi, Y.; Masaki, S.; Iwata, T.; Nakane, D.; Yasui, T.; Yuchi, A. *Anal. Chem.* **2017**, *89*, 3937–3942. DOI: [10.1021/acs.analchem.6b03754](https://doi.org/10.1021/acs.analchem.6b03754).
42. Jain, A. K.; Singh, R. K.; Jain, S.; Raisoni, J. *Transition Met. Chem.* **2008**, *33*, 243–249. DOI: <https://doi.org/10.1007/s11243-007-9022-2>.
43. Schiff, H. *Justus Liebigs Ann. Chem.* **1864**, *131*, 118–119. DOI: <https://doi.org/10.1002/jlac.18641310113>.
44. Issaadi, S.; Douadi, T.; Zouaoui, A.; Chafaa, S.; Khan, M. A.; Bouet, G. *Corros. Sci.* **2011**, *53*, 1484–1488. DOI: <https://doi.org/10.1016/j.corsci.2011.01.022>.
45. Lashgari, M.; Arshadi, M. R.; Miandari, S. *Electrochim. Acta.* **2010**, *55*, 6058–6063. DOI: <https://doi.org/10.1016/j.electacta.2010.05.066>.
46. Papic, S.; Koprivanac, N.; Grabaric, Z.; Parac-Osterman, D. *Dyes Pigment.* **1994**, *25*, 299–240. DOI: [https://doi.org/10.1016/0143-7208\(94\)85012-7](https://doi.org/10.1016/0143-7208(94)85012-7).
47. Dhar, D. N.; Taploo, C. L. *J. Sci. Ind. Res.* **1982**, *41*, 501–506.
48. Gupta, V. K.; Goyal R. N.; Pal, M. K.; Sharma, R. A. *Anal. Chim. Acta.* **2009**, *653*, 161–166. DOI: <https://doi.org/10.1016/j.aca.2009.09.008>.
49. Chaudhari, T. D.; Subnis, S. S. *Bull. Haskine Inst.* **1986**, *4*, 85–88.
50. Sharma, P. K.; Dubey, S. N. *Ind. J. Chem.* **2002**, *33A*, 1113–1115.
51. Ali, M. M.; Jesmin, M.; Salam, S. M. A.; Khanam, J. A.; Islam, M. F.; Islam, M. N. *J. Sci. Res.* **2009**, *1*, 641–646. DOI: <https://doi.org/10.3329/jsr.v1i3.2585>.
52. Fontana, R.; Marconi, P. C. R.; Caputo, A.; Gavalyan, V.B. *Molecules.* **2022**, *27*, 2740. DOI: <https://doi.org/10.3390/molecules27092740>.
53. Irawan, C.; Islamiyati, D.; Utami, A.; Putri, I. D.; Perdana Putri, R.; Wibowo, S. *Orient. J. Chem.* **2020**, *36*, 577–580. DOI: <http://dx.doi.org/10.13005/ojc/360332>.
54. Chaudhary, A.; Singh, A. *Int. J. Curr. Res. Med. Sci.* **2017**, *3*, 60–74. DOI: <http://dx.doi.org/10.22192/ijcrms.2017.03.06.009>.
55. Crespo, G. A.; Macho, S.; Rius, F. X. *Anal. Chem.* **2008**, *80*, 1316–1322. DOI: <https://doi.org/10.1021/ac071156l>.
56. Parra, E. J.; Crespo, G. A.; Riu, J.; Ruiz, A.; Rius, F. X. *Analyst.* **2009**, *134*, 1905–1910. DOI: <https://doi.org/10.1039/B908224G>.
57. Xinde, Z.; Chenggang, W.; Zhiping, L.; Zhifeng, L.; Zishen, W. *Synth. React. Inorg. Met.-Org. Chem.* **1996**, *26*, 955–966. DOI: <https://doi.org/10.1080/00945719608004346>.
58. Buck, R. P.; Lindner, E. *Pure Appl. Chem.* **1994**, *66*, 2527–2536. DOI: <https://doi.org/10.1351/pac199466122527>.
59. Umezawa, Y.; Buhlmann, P.; Umezawa, K.; Tohda, K.; Amemiya, S. *Pure Appl. Chem.* **2000**, *72*, 1851–2082. DOI: <https://doi.org/10.1351/pac200274060923>.